Spatial inhomogeneity of magnetic moments in the cobalt oxide spinel Co_3O_4

Y. Ikedo,[1] J. Sugiyama,[1] H. Nozaki,[1] H. Itahara,[1] J. H. Brewer,[2] E. J. Ansaldo,[3] G. D. Morris,[3] D. Andreica,[4] and A. Amato[4]

[1]*Toyota Central Research and Development Laboratories, Inc., Nagakute, Aich, 480-1192 Japan*

[2]*TRIUMF, CIAR, and Department of Physics and Astronomy, University of British Columbia, Vancouver, BC, V6T 1Z1 Canada*

[3]*TRIUMF, 4004 Wesbrook Mall, Vancouver, BC, V6T 2A3 Canada*

[4]*Laboratory for Muon-Spin Spectroscopy, Paul Scherrer Institut, Villigen PSI, Switzerland*

(Received 31 May 2006; revised manuscript received 8 December 2006; published 28 February 2007)

The antiferromagnetic (AF) nature of the normal spinel Co_3O_4 with Néel temperature (T_N)=30 K was investigated by means of positive muon spin rotation and relaxation (μ^+SR) techniques using a polycrystalline sample. Clear muon spin precession signals due to a quasistatic long-range AF order were found in the zero-field μ^+SR spectra below T_N. The spectra consist of two oscillating signals with frequencies at $T \to 0$ K of 80 and 60 MHz, respectively, indicating an incommensurate (IC) AF order in Co_3O_4. A possible reason for the appearance of the IC-AF order in Co_3O_4 would be local structural transitions due to a charge and/or a spin state change of Co ions.

DOI: 10.1103/PhysRevB.75.054424 PACS number(s): 76.75.+i, 75.25.+z, 75.50.Ee

I. INTRODUCTION

The magnetic properties of the cobalt oxide spinel (Co_3O_4) have been extensively studied previously by ^{59}Co nuclear magnetic resonance (^{59}Co-NMR),[1,2] magnetic susceptibility (χ),[3] neutron diffraction,[4] Mössbauer effect,[5] and heat capacity[6] (C_p) measurements, because of its unique magnetic structure and relatively strong superexchange interaction, which arises in spite of the large distance (3.89 Å) between magnetic Co ions.[4] In the last decade, both superparamagnetism and ferrimagnetism in Co_3O_4 nanoparticles have also attracted much attention not only for their fundamental interest but also for their potential applications in the realm of nanotechnology.[7–9]

The crystal structure of Co_3O_4 is a cubic normal spinel with a space group O_h^7-$Fd\bar{3}m$, lattice constant a=8.084 Å, and oxygen parameter u=0.392 at ambient temperature.[10] The charge distribution for Co_3O_4 is represented by $[Co^{2+}]_{8a}[Co_2^{3+}]_{16d}[O_4^{2-}]_{32e}$, in which 8*a* denotes the tetrahedral site and 16*d* the octahedral site surrounded by O^{2-} ions at 32*e* sites (see Fig. 1). Past work showed that Co^{3+} ions at the 16*d* site are in a diamagnetic t_{2g}^6 [low-spin (LS), S=0] state due to a strong octahedral cubic field and consequent large crystal-field splitting between t_{2g} and e_g levels in the 3*d* orbitals, while Co^{2+} ions at the 8*a* site are in a high-spin (HS) $e_g^4 t_{2g}^3$ state with S=3/2.[4] It is also well known that Co_3O_4 undergoes a magnetic transition from a high-T paramagnetic state to a low-T long-range-ordered antiferromagnetic (AF) state at T_N=30 K.

In the Co_3O_4 spinel lattice, Co^{2+} ions at the 8*a* site form a diamond lattice, which consists of two displaced face-centered-cubic (fcc) sublattices with origins at (0,0,0) and at $(\frac{1}{4},\frac{1}{4},\frac{1}{4})$. The Co^{2+} ion at (0,0,0) is thus tetrahedrally surrounded by four nearest-neighboring (NN) Co^{2+} ions. Since the four NN Co^{2+} ions form a fcc sublattice and the four Co^{2+} spins align antiparallel to the Co^{2+} spin at (0,0,0), which belongs to the other fcc sublattice, the spin arrangement in each sublattice is ferromagnetic (FM) but it is AF between adjacent sublattices.[4] As a result, the magnetic space group of Co_3O_4 changes from high-T O_h^7-$Fd\bar{3}m$ to low-T T_d^2-$F\bar{4}3m$ at T_N, although no structural phase transition was found down to the lowest T measured.[4] In this paper, we use site notations for $Fd\bar{3}m$ even in the AF state for simplicity.

One of our motivations for investigating the magnetism of Co_3O_4 is the fact that Co_3O_4 is the parent compound for layered cobalt oxides such as Na_xCoO_2 (Ref. 11), $[Ca_2CoO_3]_{0.62}^{RS}[CoO_2]$ (Ref. 12), and $[Ca_2Co_{4/3}Cu_{2/3}O_4]_{0.62}^{RS}[CoO_2]$ (Ref. 13) (RS denotes a rocksalt-type sublattice), which exhibit metallic conductivity and an extraordinarily large thermopower. These features make them promising candidates as the basic material for thermoelectric power generation systems. In order to understand the origin of good thermoelectric performance in these layered cobalt oxides, we previously carried out positive muon spin rotation and relaxation (μ^+SR) experiments on these materials,[14–22] and found that a short-range incommensurate spin-density-wave (IC-SDW) order appears below 100 K ($=T_{SDW}^{on}$) and a long-range order forms below 30 K ($=T_{SDW}^{end}$) for $[Ca_2CoO_3]_{0.62}^{RS}[CoO_2]$,[18] and T_{SDW}^{on}=200 K and T_{SDW}^{end}=140 K for $[Ca_2Co_{4/3}Cu_{2/3}O_4]_{0.62}^{RS}(CoO_2)$.[20] Since a long-range commensurate AF order is also observed for

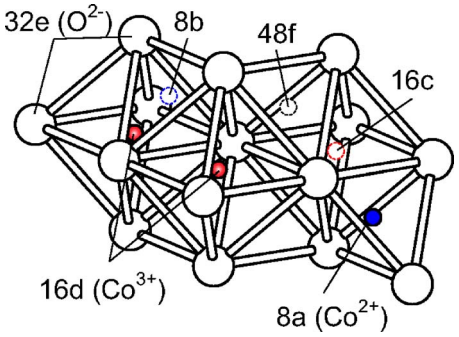

FIG. 1. (Color online) The crystal structure of Co_3O_4. 8*a* (tetrahedron) and 16*d* (octahedron) sites are occupied by Co^{2+} and Co^{3+} ions, respectively. 8*b* and 48*f* sites are empty tetrahedra and the 16*c* site is empty octahedron.

$Na_{0.75}CoO_2$,[15] we proposed that the IC-SDW lies not in the rocksalt-type $[Ca_2CoO_3]$ and/or $[Ca_2Co_{4/3}Cu_{2/3}O_4]$ sublattice but in the CoO_2 planes.

More recent μ^+SR and neutron scattering results on improved single-crystal samples, however, indicate that the magnetic ordering is more complex than postulated above, because of the following.

(i) The magnetic order for Na_xCoO_2 with $x=0.75$ and 0.82 was found to be *A*-type AF—i.e., FM in the CoO_2 plane but AF between adjacent CoO_2 planes, by recent neutron experiments.[23,24]

(ii) The internal magnetic field at $T\rightarrow 0$ K ($H_{\text{int,0 K}}$) corresponds to a muon spin precession frequency of 54 MHz for $[Ca_2CoO_3]^{RS}_{0.62}[CoO_2]$ (Ref. 18) and 60 MHz for $[Ca_2Co_{4/3}Cu_{2/3}O_4]^{RS}_{0.62}[CoO_2]$,[20] whereas it is 8 MHz for $LiCoO_2$,[22] $\leqslant$3 MHz for Na_xCoO_2,[15] and $<$1.5 MHz for $K_{0.49}CoO_2$.[21]

(iii) The layered cobalt oxides $[Sr_{2-x}Pb_xBi_2O_4]_{0.5}[CoO_2]$, which lack Co ions in the rocksalt-type sublattice, do not exhibit IC-SDW order but only a static Kubo-Toyabe muon spin relaxation below $\sim$3 K, while the resistivity-*T* curves show a broad minimum around 60 K, which was thought to indicate the appearance of the IC-SDW order in that system.[25]

(iv) According to other past μ^+SR work, $\nu(H_{\text{int}})$ $\sim$55 MHz for rocksalt CoO ($T_N=290$ K).[26]

Since implanted muons in oxides bind preferentially with O^{2-} ions to form a O-μ^+ bond (similar to the O-H^+ hydrogen bond), the magnitude of H_{int} detected by μ^+SR is determined by both the distance (bond length) between Co and O ions ($d_{\text{Co-O}}$) and the magnitude of the Co spin—i.e., moment. In $[Ca_2CoO_3]^{RS}_{0.62}[CoO_2]$, $d_{\text{Co-O}}$ was reported to range from 1.8 to 2.0 Å in the $[CoO_2]$ sublattice and from 1.6 to 2.7 Å in the $[Ca_2CoO_3]$ sublattice.[27] The large variation in $d_{\text{Co-O}}$ in $[Ca_2CoO_3]$ is caused by a misfit between the two sublattices. Although the charge distribution of Co ions in $[Ca_2CoO_3]^{RS}_{0.62}[CoO_2]$ and/or $[Ca_2Co_{4/3}Cu_{2/3}O_4]^{RS}_{0.62}[CoO_2]$ is still unknown, the longer $d_{\text{Co-O}}$ in $[Ca_2CoO_3]$ than in $[CoO_2]$ and common transport properties of the layered cobalt oxides suggest that both Co^{3+} and Co^{4+} coexist in $[CoO_2]$, whereas the average valence is almost 3+ for Co ions in the RS sublattice.

In the Co_3O_4 spinel, on the other hand, $d_{\text{Co}^{3+}\text{-O}}$ is $\sim$1.92 Å and $d_{\text{Co}^{2+}\text{-O}}\sim$1.93 Å. The spinel Co_3O_4 is considered to be a cation-deficient rocksalt; that is, O^{2-} ions at the 32*e* site and Co^{3+} ions at the 16*d* site form an RS lattice together with the vacant 16*c* site, while Co^{2+} ions locate at the interstitial 8*a* site. By comparison with the layered cobalt oxides, Co_3O_4 possesses a simple structure with a well-known charge distribution in the lattice. We therefore initiated the present study of the magnetic properties of Co_3O_4 in order to obtain more insights into the nature of the layered cobalt oxides.

Furthermore, μ^+SR, as it is very sensitive to the local magnetic environment,[26,28,29] provides unique information on spatially inhomogeneous long-range ordering, such as an IC-spin-density-wave (SDW) state.[30,31] This is because the local magnetic field at a crystallographic μ^+ site varies depending on the spatial inhomogeneity, naturally generating a wide field distribution and as a result a rapidly relaxing oscillation. In model AF cases, on the other hand, a long-lived oscillating signal is normally observed; i.e., the relaxation rate is very small, because the local magnetic field is in principle identical for each μ^+ site. In this paper, we report on both weak (relative to the spontaneous internal fields in the ordered state) transverse-field (wTF-)μ^+SR and zero-field (ZF-)μ^+SR for a polycrystalline Co_3O_4 sample at temperatures between 1.8 and 60 K, with the aim of elucidating the nature of the AF phase of Co_3O_4 with $T_N=30$ K.

II. EXPERIMENT

A polycrystalline sample of Co_3O_4 was synthesized by a tape-casting method using β-$Co(OH)_2$ crystal platelets as a starting material. The sample was sintered at 1200 K for 2 h in an O_2 atmosphere followed by annealing in an O_2 gas flow. The spinel structure of the sample was confirmed by x-ray diffraction measurements. The diffraction pattern showed only peaks due to Co_3O_4 spinel structure.

Magnetic susceptibility was measured using a superconducting quantum interference device (SQUID) magnetometer (MPMS, Quantum Design) at temperatures between 400 and 5 K. Heat capacity was measured using relaxation technique (PPMS, Quantum Design) in the temperature range between 300 and 1.9 K.

The μ^+SR experiments were performed on the surface muon beamline of M20 at TRIUMF and the πE1 beamline at PSI using the instrument Dolly. Experimental setup and techniques are described elsewhere.[32]

III. RESULTS

A. Magnetic susceptibility and specific heat

The magnetic susceptibility χ of the polycrystalline Co_3O_4 sample was measured in field cooling mode with 10 kOe at temperatures from 400 to 5 K. Figure 2 shows the temperature dependence of (a) χ and (b) χ^{-1}. The inset of Fig. 2(a) shows the slope of χ ($d\chi/dT$) as a function of *T*. The $\chi(T)$ curve exhibits a broad maximum at around 40 K, whereas the $d\chi/dT$ shows a sharp peak at 29 K. Above 40 K, χ decreases monotonically with increasing *T*, while χ^{-1} increases almost linearly with increasing *T*, indicating a Curie-Weiss paramagnetic behavior. Indeed, the *T* dependence of χ above 100 K is well represented by

$$\chi(T)=\chi_0+C/(T-\Theta_p), \tag{1}$$

where χ_0 is the temperature-independent susceptibility, *C* is the Curie-Weiss constant, and Θ_p is the paramagnetic Curie temperature. The fit for the $\chi(T)$ curve using Eq. (1) over the *T* range above 100 K yields $\Theta_p=95\pm2$ K, $\chi_0=(1.86\pm0.07)\times10^{-3}$ emu/(mol Co^{2+}), and $C=2.86\pm0.04$ K emu/(mol Co^{2+}). The effective magnetic moment per mol Co (μ_{eff}) is calculated by using the formula $C=N\mu^2_{\text{eff}}/3k_B$, where *N* is the number density of Co^{2+} ions per mol and k_B is the Boltzmann constant. We obtain $\mu_{\text{eff}}=(4.79\pm0.02)\mu_B$, where μ_B is the Bohr magneton.

The current results are very consistent with the data estimated from the $\chi(T)$ curve below 300 K: that is, Θ_p

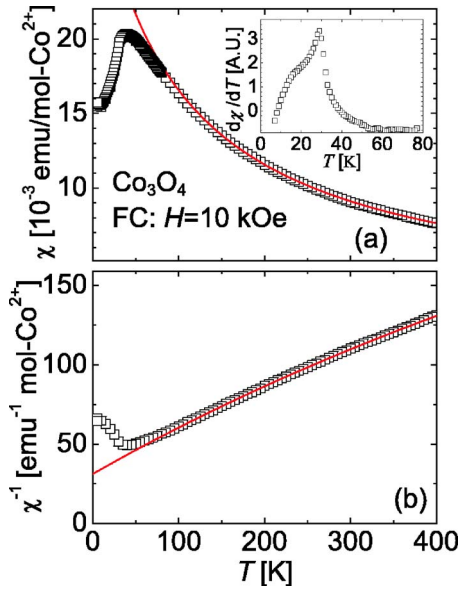

FIG. 2. (Color online) Temperature dependences of (a) magnetic susceptibility χ and (b) inverse magnetic susceptibility χ^{-1} for Co_3O_4. Solid lines represent the fit results using Eq. (1). The inset of (a) shows slope of χ ($d\chi/dT$) as a function of T.

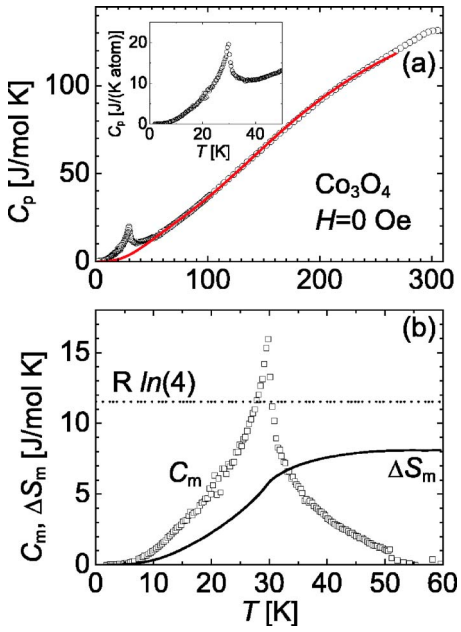

FIG. 3. (Color online) Temperature dependences of (a) C_p and (b) C_m. The solid line in (a) indicates the fit result using Eq. (2) and in (b) the magnetic entropy calculated using Eq. (3). $R\ln(4)$ is the expected value of the magnetic entropy for $S=3/2$ system. The inset of (a) shows the magnification of the $C_p(T)$ curve in the vicinity of T_N.

$=108$ K and $\mu_{eff}=4.74\mu_B$.[33] It should be, however, noted that Cosse reported $\Theta_p=53$ K and $\mu_{eff}=4.14\mu_B$ from a χ measurement up to 1000 K.[3] The discrepancy between the data is probably due to the spin-state transition around 600 K—i.e., the spin state of Co^{3+} ions at the 16*d* site changes from the low-T LS state ($S=0$) to the high-T HS state ($S=2$).[34] In order to explain the nature of Co_3O_4 at low T, which we are primarily interested in, the data below 600 K are therefore considered to be suitable. In addition, μ_{eff} of the spinel $CoAl_2O_4$ ($4.65\mu_B$),[35] in which Co^{2+} ions locate only at the 8*a* site, is in good agreement with the present result, supporting the present determination of Θ_p and μ_{eff} for Co_3O_4. Assuming that Co^{2+} ions are responsible for the Curie-Weiss paramagnetic behavior, the estimated $\mu_{eff}=4.79\mu_B$ is greater than the spin-only value for free Co^{2+} ions ($3.88\mu_B$), indicating a contribution of the spin-orbit coupling of Co^{2+}, as explained by Roth.[4]

Figure 3(a) shows the T dependence of C_p in zero field in the T range between 400 and 1.9 K. The inset of Fig. 3(a) is a magnification of the $C_p(T)$ curve around 30 K. A clear λ-type peak with the maximum at 29.8 ± 0.3 K in the $C_p(T)$ curve yields the correct value of T_N for the present sample. For Co_3O_4, C_p has both phonon C_{ph} and magnetic C_m contributions. In order to estimate C_m, we employ the combined Einstein-Debye model for C_{ph} as[6,35]

$$C_{ph}=9Rx_D^{-3}\int_0^{x_D}\frac{x^4e^x}{(e^x-1)^2}dx+R\sum_{i=1}^{2}a_i\frac{x_{E_i}^2e^{x_{E_i}}}{(e_{E_i}^x-1)^2}. \quad (2)$$

The first term represents the Debye-type phonon contribution (acoustic mode) and the second term the Einstein-type contribution (two optical modes). Both $x_D=\Theta_D/T$ and $x_{E_i}=\Theta_{E_i}/T$ are the reduced T^{-1} for the Debye temperature (Θ_D) and the Einstein temperature (Θ_{E_i}), respectively. $R=8.31$ J/(mol K) is the molar gas constant, and a_i is the number of degree of freedom for each Einstein mode; for the cubic spinel, $a_1=3$ and $a_2=15$.[6] Above 50 K, the $C_p(T)$ curve is well fitted by Eq. (2), and as a result we obtain $\Theta_D=234\pm3$ K, $\Theta_{E_1}=311\pm4$ K, and $\Theta_{E_2}=707\pm1$ K. Then the $C_m(T)$ curve is calculated by subtracting $C_{ph}(T)$ from the measured $C_p(T)$ curve [see Fig. 3(b)]. The $C_m(T)$ curve naturally exhibits a sharp maximum at $T_N=29.8\pm0.3$ K. The entropy change from a magnetically ordered state to a disordered state (ΔS_m) is calculated by the formula

$$\Delta S_m(T)=\int_0^T\frac{C_m(T)}{T}dT. \quad (3)$$

Figure 3(b) also shows the $\Delta S_m(T)$ curve estimated using Eq. (3) and the magnetic entropy change expected for the $S=3/2$ system—i.e., $R\ln(2S+1)=11.5$ J K^{-1} mol^{-1}, while the measured ΔS_m is estimated as 8.1 J K^{-1} mol^{-1} even at 60 K. The difference is probably due to grain boundary effects in the polycrystalline sample and/or the difficulty to fit C_{ph}, as reported in Ref. 6.

B. Weak transverse field μ^+SR

Figure 4 shows wTF-μ^+SR spectra for Co_3O_4 obtained at 60 K (squares), 30 K (triangles), and 8 K (circles) in a magnetic field of $H=50$ Oe, where $\vec{H}$ is perpendicular to the initial muon spin direction ($\vec{S}_\mu$). A clear muon oscillation signal due to the external field is observed at 60 K. As T

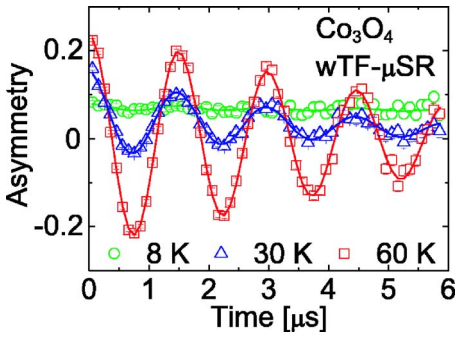

FIG. 4. (Color online) Weak transverse field (wTF-)μ^+SR time spectra for Co_3O_4 at 60 K (squares), 30 K (triangles), and 8 K (circles). The magnitude of the applied wTF is 50 Oe.

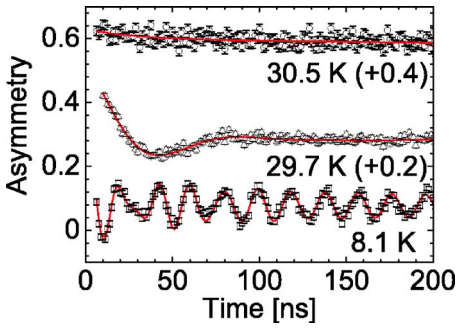

FIG. 6. (Color online) Early times part of ZF-μ^+SR spectra for Co_3O_4 at above and below T_N=30 K. The full spectra extend up to 10 μs. Solid lines represent fits using Eq. (5)

decreases below 30 K, the amplitude of this signal decreases drastically and at 8 K there remains only a nonoscillatory, slowly relaxing signal. Actually the wTF-μ^+SR spectra were well fitted in the time domain using a combination of an exponentially relaxing cosine oscillation, due to the external field, and an exponentially relaxing nonoscillatory signal caused by the appearance of random internal fields in the ordered state:

$$A_0 P(t) = A_{\mathrm{TF}} \exp(-\lambda_{\mathrm{TF}} t)\cos(\omega_\mu t + \phi) + A_{\mathrm{slow}} \exp(-\lambda_{\mathrm{slow}} t), \tag{4}$$

where A_0 is the total initial asymmetry, $P(t)$ is the muon spin polarization function, ω_μ is the muon Larmor frequency, ϕ is the initial phase of the muon precession, and A_n and λ_n (n =TF and slow) are asymmetries and relaxation rates of the two signals.

Figures 5(a) and 5(b) show the T dependence of A_n and λ_n for Co_3O_4 below 60 K. Above 30 K, A_{TF} is almost constant at its maximum value (~0.24), showing that the whole sample is paramagnetic. As T decreases from 30 K, A_{TF} suddenly decreases and vanishes below 29 K, while A_{slow} appears at 30 K and seems to level off to the constant value (~0.075) below 20 K. As T decreases from 60 K, λ_{TF} is also

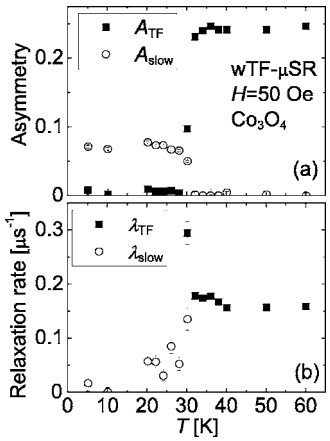

FIG. 5. Temperature dependences of (a) asymmetries (A_{TF} and A_{slow}) and (b) relaxation rates (λ_{TF} and λ_{slow}) for Co_3O_4. The data were obtained by fitting the wTF-μ^+SR spectra using Eq. (4).

independent of T down to 40 K, then slightly increases, leaps by 0.1 μs^{-1} at 30 K, and then disappears with further lowering T below 30 K. λ_{TF} above 40 K is mainly due to the nuclear magnetic moments of ^{59}Co nuclei in the paramagnetic state, while the slight increase below 40 K would imply the formation of short-range AF order of Co ionic moments. On the other hand, λ_{slow} decreases monotonically with decreasing T below the transition, showing typical critical behavior for a transition at T_N.

These indicate a sharp transition to a long-range AF order which completes below 30 K—that is, T_N=30 K, which is very consistent with the result of the C_p measurement. Moreover, A_{slow}(5 K) corresponds to 1/3 of the maximum value of A_{TF}, as expected for a powder sample since 1/3 of the muons experience the internal field component parallel to $\vec{S}_\mu$ (part of the signal known as the "1/3 tail"). The remaining 2/3 muon spins oscillate very rapidly due to the components of the internal field perpendicular to $\vec{S}_\mu$, but such oscillating signals are averaged out within the time resolution in Fig. 4 and do not contribute to the signal at longer times. Since A_{TF} is proportional to the volume fraction of paramagnetic phases in the sample, the wTF results show that the whole sample volume enters into the AF phase.

C. Zero-field μ^+RS

In order to investigate the internal magnetic field ($\vec{H}_{\mathrm{int}}$) of the AF phase for Co_3O_4 in detail, ZF-μ^+SR experiments were performed below 31 K. Figure 6 shows ZF-μ^+SR time spectra at 30.5 K (top), 29.7 K (middle), and 8.1 K (bottom). A clear spontaneous muon spin oscillatory signal due to a quasistatic $\vec{H}_{\mathrm{int}}$ is observed below 29.7 K ("quasistatic" means static at least within the time scale of μ^+SR—i.e. up to ~10 μs), whereas there is no oscillation signal at 30.5 K, further indicating the appearance of a long-range AF-ordered state below 29.7 K.

The Fourier transforms of ZF-μ^+SR time spectra clearly show two distinct frequency components in each spectrum (see Fig. 7). The spectrum at 8 K consists of a main peak at ν_2=51.6 MHz and a second broad weaker maximum at ν_1 =72.7 MHz, corresponding to $H_{\mathrm{int},2}$=3.8 kOe and $H_{\mathrm{int},1}$ =5.4 kOe, respectively. Both ν_1 and ν_2 monotonically de-

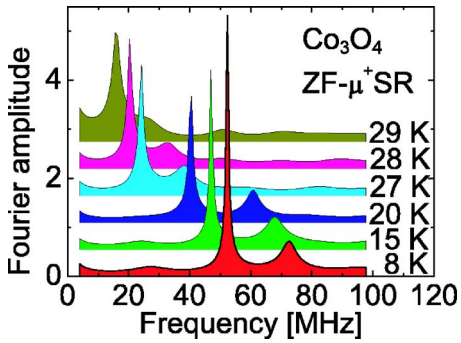

FIG. 7. (Color online) Fourier amplitude of ZF-μ^+SR spectra at several temperatures below T_N.

crease with increasing T and disappear simultaneously at 30 K.

The full widths at half maximum (FWHM) of the two peaks at ν_1 and ν_2 increase with increasing T, and the former is broader than the latter in the whole T range measured. In the layered cobalt oxides, such as Na_xCoO_2 and $[Ca_2CoO_3]^{RS}_{0.62}[CoO_2]$, coexisting Co^{3+} and Co^{4+} ions in the CoO_2 planes naturally induce the wide distribution of H_{int}. On the contrary, in the Co_3O_4 spinel, Co^{2+} ions locate only at the $8a$ site. As a result, the FWHM (T=8 K) at ν_1 is 6.0 MHz and at ν_2 1.6 MHz, respectively, while the FWHM of the main peak (ν=55 MHz) for $[Ca_2CoO_3]^{RS}_{0.62}[CoO_2]$ is about 20 MHz at 2.5 K and for $Na_{0.75}CoO_2$ 1 MHz (ν =3.3 MHz) at 2.5 K. This shows that the distribution of H_{int} in Co_3O_4 is rather small compared with those in the layered cobalt oxides, as expected.

There are two possible reasons for the appearance of the two oscillatory components in the ZF time spectra: namely, the presence of two magnetically inequivalent μ^+ sites and an incommensurate (IC) magnetic order in the AF phase of Co_3O_4. In the former case, a phenomenological relaxation function for the oscillatory components in the ZF time spectrum is a combination of two exponentially damped cosine signals, $\Sigma A_n \exp(-\lambda_n t)\cos(2\pi\nu_n t+\phi_n)$ (n=1 and 2, $\nu_1 > \nu_2$). Actually, the ZF time spectra for Co_3O_4 below T_N are well fitted by this phenomenological function except that the fit results exhibit a large negative phase shift for both oscillatory signals; i.e., the delay of the initial phases are $\phi_1 = -70° \pm 5°$ and $\phi_2 = -48° \pm 4°$ at 8 K. This indicates the appearance of the IC magnetic order below T_N for Co_3O_4, because ϕ should be zero for commensurate (C-)AF order.[36] Furthermore, as T decreases from 30 K, A_1 (A_2) increases (decreases) monotonically with T from 0.06 (0.10) at 30 K to 0.11 (0.06) at 8 K. In order to explain the $A_1(T)$ and $A_2(T)$ curves, one would have to assume the existence of two muon sites and a situation whereby the population of μ^+ at each site changes monotonically with T. Such behavior is very unlikely to occur at low T.

The ZF time spectra were therefore fitted with the following formula:[37]

$$A_0P(t) = A_1J_0(2\pi\nu_1 t)\exp(-\lambda_1 t) + A_2\exp(-\lambda_2 t) \times\cos(2\pi\nu_2 t+\phi) + A_{\text{slow }1}\exp(-\lambda_{\text{slow }1} t) + A_{\text{slow }2}\exp(-\lambda_{\text{slow }2} t),$$

$$\nu_1 > \nu_2, \tag{5}$$

where A_0 is the total initial asymmetry, $P(t)$ is the muon polarization function, A_n, λ_n, and ν_n (n=1 and 2) are the asymmetries, relaxation rates, and oscillation frequencies of the two oscillating signals, respectively, ϕ is the initial phase of the exponentially damped term, and $A_{\text{slow},n}$ and $\lambda_{\text{slow},n}$ (n =1 and 2) are the asymmetries and relaxation rates of the non-oscillating signals, respectively. $J_0(2\pi\nu_1 t)$ is the zeroth-order Bessel function of the first kind. This is because according to the lattice sum calculation, a generalized IC field distribution at the muon site H is given by[30,37,38]

$$P(H) = \frac{2}{\pi}\frac{H}{\sqrt{(H_1^2-H^2)(H^2-H_2^2)}},$$

$$H_2 < H < H_1, \tag{6}$$

where $2\pi\nu_1 = \gamma_\mu H_1$ and $2\pi\nu_2 = \gamma_\mu H_2$ (γ_μ is the muon gyromagnetic ratio). Since Eq. (6) represents the field distribution in a frequency domain, Eq. (6) is unavailable to fit ZF-μ^+SR time spectra. On the other hand, the sum of $J_0(2\pi\nu t)$ and the cosine function, which corresponds to the first two terms in Eq. (5), is known to well represent the fine spectrum of $P(H)$. We thus used Eq. (5) to fit the ZF-μ^+SR spectra of Co_3O_4. The two nonoscillating components in Eq. (5) correspond to the "1/3 tail," as described in the previous section on wTF-μ^+SR results.

Figure 8 shows the T dependences of (a) λ_n, (b) A_1+A_2 and $A_{\text{slow1}}+A_{\text{slow2}}$, and (c) ν_n and $\Delta\nu=\nu_1-\nu_2$ of the two oscillating signals (n=1 and 2) obtained by the fitting results using Eq. (5). As T decreases from 30 K, both λ_1 and λ_2 rapidly decrease with decreasing slope and reach their minima below ~15 K. This is reasonably explained by the critical phenomenon in the magnetically ordered system at the vicinity of T_N.

A_1+A_2 is almost T independent below T_N and levels off to its maximum value (~0.15) for a magnetic powder sample. $A_{\text{slow1}}+A_{\text{slow2}}$ is also T independent below T_N and levels off to half the value of A_1+A_2 (~0.08). This indicates that $A_{\text{slow1}}+A_{\text{slow2}}$ represent the "1/3 tail," which is consistent with the result of wTF-μSR. The result is further evidence supporting the conjecture that the whole sample enters into the IC-AF order phase below T_N.

The two $\nu_n(T)$ curves exhibit a similar T dependence [see Fig. 8(c)]. As T decreases from 31 K, both ν_1 and ν_2 suddenly appear at 30 K and increase with decreasing T, with decreasing slope. At the vicinity of T_N, $\Delta\nu$ rapidly increases with decreasing T and seems to level off to ~20 MHz below 20 K. Since $\Delta\nu$ measures the field distribution of the IC order, this implies that the IC AF structure of Co_3O_4 is completed at 20 K. This is consistent with the result of the T dependences of the λ_n as described above.

The other parameters A_{slow1}, A_{slow2}, λ_{slow1}, and λ_{slow2} lack T dependence below T_N, indicating that the implanted muon does not change the site at least in the time scale of the muon lifetime. The $\phi(T)$ curve is independent of T with $\phi \sim 10°$ at

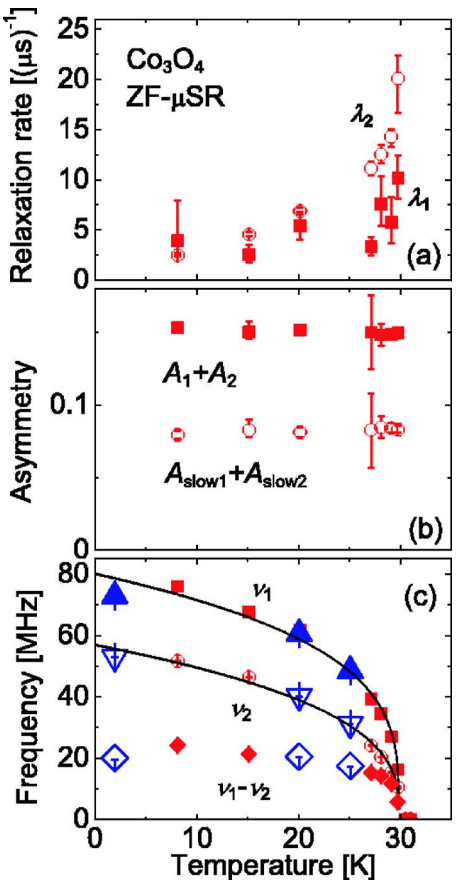

FIG. 8. (Color online) Temperature dependences of (a) λ_n, (b) A_1+A_2 and $A_{slow1}+A_{slow2}$, and (c) ν_n ($n=1$ and 2) and $\Delta\nu=\nu_1-\nu_2$. These results were obtained by fitting the ZF-μ^+SR spectra with Eq. (5). Solid curves are guide to the eye. ▲, ▽, ◇ and data obtained at TRIUMF and ■, ○, and ◆ and at PSI.

whole temperatures measured. This phase shift is due to the rotation of the initial muon spin direction by 10° to avoid direct positrons from the muon source.

IV. DISCUSSION

A. Origin of incommensurate order

Here, we discuss the origin of the IC-AF order in Co_3O_4. To begin with, the magnetic interaction between Co^{2+} ions at the 8*a* site is known to proceed via multiple exchange paths involving several Co^{2+}-O-Co^{3+}-O-Co^{2+} bonds (see Fig. 1).[4] Additionally, among related materials, $CoAl_2O_4$ lacks a magnetically ordered state even at 4 K,[39] while $CoRh_2O_4$, in which Rh^{3+} is in the $4d^6$ configuration of LS state ($S=0$), exhibits a long-range AF order below $T_N=27$ K.[40] This suggests that the vacant e_g orbitals at the 16*d* site play an important role in the AF order in Co_3O_4. We therefore need to take into account not only the nature of the magnetic Co^{2+} ions at the 8*a* site but also the charge and/or spin fluctuations of Co^{3+} at the 16*d* site for explaining the origin of the IC-AF order.

Since the exchange path through three intervening ions produces a relatively weak superexchange interaction, which is responsible for the AF ordering of Co_3O_4, either a slight local structural distortion around Co ions or the change in charge and spin of Co^{3+} would alter the overlap between the orbitals of Co^{3+} and O^{2-}, resulting in a modulation of the local internal magnetic field of Co_3O_4.

According to a recent neutron diffraction study for a cubic spinel $MnSc_2S_4=[Mn^{2+}]_{8a}[Sc_2^{3+}]_{16d}[S_4^{2-}]_{32e}$ with $T_N=2.3$ K[41] an IC-SDW order with a spiral magnetic structure was found below T_N, although there are no structural phase transitions down to 1.5 K. The origin of the IC-SDW order in $MnSc_2S_4$ was proposed as a local structural transition due to spin-driven Jahn-Teller (JT) effects below T_N. Such a transition was, however, considered to be undetectable, because the distortion is probably far beyond the resolution of the current neutron diffraction technique.

A similar scenario would be applicable for Co_3O_4, which also keeps a cubic symmetry down to 4.2 K,[4] if Co ions are JT active. The possible reactions in the AF phase of Co_3O_4 are therefore as follows.

(i) Spin-state transition of Co^{3+} ions at the 16*d* site: $Co^{3+}(LS,S=0)\rightarrow Co^{3+}$ (HS, $S=1$ or $S=2$).

(ii) Charge disproportionation of Co^{3+} ions at the 16*d* site into Co^{2+} and Co^{4+} ions: Co^{3+} (LS)$\rightarrow Co^{2+}$ (HS,$S=3/2$) $+Co^{4+}$ ($S=1/2$).

(iii) Exchange of Co^{2+} ion at the 8*a* site with Co^{3+} ion at the 16*d* site: Co^{2+} ($8a,S=3/2$)$+Co^{3+}$ ($16d,S=0$)$\rightarrow Co^{3+}$ ($8a,S=2$)$+Co^{2+}$ ($16d,S=3/2$).

All the reactions listed above are assigned to an electron transfer process between Co ions with activation energies ranging from 0.3 to 0.7 eV.[34] The above reactions are thus likely to occur locally even at low T and, as a result, induce a local JT distortion in the CoO_6 octahedra. Such distortion naturally leads to a fluctuation of the distance between Co^{2+} ions and μ^+. We should here note that, although there is no evidence for IC-SDW order in the past neutron powder diffraction measurements, it is not impossible but very difficult to detect the IC-SDW order by neutron. This is because the IC modulation reduces the intensity of magnetic Bragg peaks. In order to further understanding of the origin of the inhomogeneity, additional μ^+SR experiments are required using single-crystal samples of Co_3O_4 to determine the μ^+ sites more precisely and to know the relationship between H_{int} and the easy axis of magnetization.

B. Comparison with layered cobalt oxides

In earlier μ^+SR work, two major precessing signals with $\nu_n(0\text{ K})=54$ and 78 MHz, plus a minor signal at 150 MHz, were observed in a rocksalt-type CoO ($Co^{2+}O^{2-}$) crystal,[26] comparable to the present experimental values of $\nu_n(0\text{ K})=60$ and 80 MHz for the $[Co^{2+}]_{8a}[Co_2^{3+}]_{16d}[O_4^{2-}]_{32e}$ spinel. In the AF phase of CoO below $T_N=290$ K, the spins of Co^{2+} ions align parallel to each other on (111) planes, but with antiparallel spin directions in alternate (111) planes. It is therefore very surprising that H_{int} detected by μ^+ for CoO are almost the same as for Co_3O_4, in spite of the fact that the magnetic structure of CoO is so different from that of Co_3O_4. This could suggest the existence of Co^{2+} ions in the 16*d* site in Co_3O_4, as in the case for the well-known Fe_3O_4

$=[Fe^{3+}]_{8a}[Fe^{2+}Fe^{3+}]_{16d}[O_4^{2-}]_{32e}$ case. However, Co^{2+} ions are most unlikely to exist in $[Ca_2CoO_3]^{RS}_{0.62}[CoO_2]$ based on χ measurements,[42] a bond-valence-sum calculation using the structural refinement data,[43] and a photoelectron spectroscopic analysis at ambient temperature.[44] Nevertheless, assuming that a charge disproportionation of Co^{3+} ions ($2Co^{3+} \rightarrow Co^{2+} + Co^{4+}$) occurs in the CoO_2 planes at low T as in the case for $LiCoO_2$,[22] it would be reasonable that the IC-SDW with $\nu(0\ K) = 54$ MHz exists in the CoO_2 planes in $[Ca_2CoO_3]^{RS}_{0.62}[CoO_2]$. Although the current μ^+SR results on Co_3O_4 do not provide crucial information concerning the position of the IC-SDW in the layered cobalt oxides, indirect evidence, if Co^{2+} ions exist in the 16*d* octahedral site, still seems to support that the IC-SDW lies in the CoO_2 planes.

V. SUMMARY

The magnetic properties of Co_3O_4 below T_N were studied in wTF- and ZF-μ^+SR experiments, together with magnetic susceptibility and heat capacity measurements. Spontaneous muon spin precession signals with two different frequencies 77 ± 4 and 56 ± 3 MHz ($T \rightarrow 0$) were observed in ZF-μ^+SR spectra below 30 K, both with sizable inhomogeneous broadening. The precise analyses of the ZF spectra also suggested the formation of an incommensurate antiferromagnetic order below T_N. Although the origin of the inhomogeneity of the magnetic moment in the AF order state is not fully understood, it could be caused by a slight structural distortion together with a spin and/or charge state transition of Co^{3+} ions at the 16*d* site. Experiments on not only a single crystal Co_3O_4 but also related materials, such as, $CoRh_2O_4$, $ZnCo_2O_4$ (diamagnetic ions at 8*a* sites), and $CoAl_2O_4$ (diamagnetic ions at 16*d* sites), help to elucidate the role of Co^{3+} ions at the 16*d* site on the long-range AF order.

ACKNOWLEDGMENTS

This work was performed at both TRIUMF, Vancouver, Canada and the Swiss Muon Source, Paul Sherrer Institut, Villigen, Switzerland. We thank S. R. Kreitzmann, B. Hitti, and D. J. Arseneau of TRIUMF, P. Russo of Columbia University, and LMU staff of PSI for help with the μ^+SR experiments. This work was partially (J.H.B.) supported at UBC by CIAR, NSERC of Canada, and at TRIUMF by NRC of Canada.

[1] K. Miyatani, K. Kohn, H. Kamimura, and S. Iida, J. Phys. Soc. Jpn. **21**, 464 (1966).
[2] H. Kamimura, J. Phys. Soc. Jpn. **21**, 484 (1966).
[3] P. Cosse, J. Inorg. Nucl. Chem. **8**, 483 (1958).
[4] W. L. Roth, J. Phys. Chem. Solids **25**, 1 (1964).
[5] W. Kundig, M. Kobelt, H. Appel, G. Constabaris, and R. H. Lindquist, J. Phys. Chem. Solids **30**, 819 (1969).
[6] L. M. Khriplovich, E. V. Kholopov, and I. E. Paukov, J. Chem. Thermodyn. **14**, 207 (1982).
[7] Y. Ichiyanagi, Y. Kimishima, and S. Yamada, J. Magn. Magn. Mater. **272-276**, e1245 (2004).
[8] B. Pejova, A. Isahi, M. Najdoski, and I. Grozdanov, Mater. Res. Bull. **36**, 161 (2001).
[9] C. Nethravathi, S. Sen, N. Ravishankar, M. Rajamathi, C. Pietzonka, and B. Harbrecht, J. Phys. Chem. B **109**, 11468 (2005).
[10] W. L. Smith and A. D. Hobson, Acta Crystallogr., Sect. B: Struct. Crystallogr. Cryst. Chem. **29**, 362 (1973).
[11] J. Molenda, C. Delmas, P. Dordor, and A. Stoklosa, Solid State Ionics **12**, 473 (1989).
[12] R. Funahashi, I. Matsubara, H. Ikuta, T. Takenouchi, U. Mizukami, and S. Sodeoka, Jpn. J. Appl. Phys., Part 2 **39**, L1127 (2000).
[13] Y. Miyazaki, T. Miura, Y. Ono, and T. Kajitani, Jpn. J. Appl. Phys., Part 2 **41**, L849 (2002).
[14] J. Sugiyama, J. H. Brewer, E. J. Ansaldo, H. Itahara, T. Tani, M. Mikami, Y. Mori, T. Sasaki, S. Hebert, and A. Maignan, Phys. Rev. Lett. **92**, 017602 (2004).
[15] J. Sugiyama, H. Itahara, J. H. Brewer, E. J. Ansaldo, T. Motohashi, M. Karppinen, and H. Yamauchi, Phys. Rev. B **67**, 214420 (2003).
[16] J. Sugiyama, J. H. Brewer, E. J. Ansaldo, B. Hitti, M. Mikami, Y. Mori, and T. Sasaki, Phys. Rev. B **69**, 214423 (2004).
[17] J. Sugiyama, H. Itahara, T. Tani, J. H. Brewer, and E. J. Ansaldo, Phys. Rev. B **66**, 134413 (2002).
[18] J. Sugiyama, J. H. Brewer, E. J. Ansaldo, H. Itahara, K. Dohmae, Y. Seno, C. Xia, and T. Tani, Phys. Rev. B **68**, 134423 (2003).
[19] J. Sugiyama, H. Nozaki, J. H. Brewer, E. J. Ansaldo, T. Takami, H. Ikuta, and U. Mizutani, Phys. Rev. B **72**, 064418 (2005).
[20] J. Sugiyama, J. H. Brewer, E. J. Ansaldo, H. Itahara, K. Dohmae, C. Xia, Y. Seno, B. Hitti, and T. Tani, J. Phys.: Condens. Matter **15**, 8619 (2003).
[21] J. Sugiyama, H. Nozaki, Y. Ikedo, K. Mukai, J. H. Brewer, E. J. Ansaldo, G. D. Morris, D. Andreica, A. Amato, T. Fujii, and A. Asamitsu, Phys. Rev. Lett. **96**, 037206 (2006).
[22] J. Sugiyama, H. Nozaki, J. H. Brewer, E. J. Ansaldo, G. D. Morris, and C. Delmas, Phys. Rev. B **72**, 144424 (2005).
[23] L. M. Helme, A. T. Boothroyd, R. Coldea, D. Prabhakaran, D. A. Tennant, A. Hiess, and J. Kulda, Phys. Rev. Lett. **94**, 157206 (2005).
[24] S. P. Bayrakci, I. Mirebeau, P. Bourges, Y. Sidis, M. Enderle, J. Mesot, D. P. Chen, C. T. Lin, and B. Keimer, Phys. Rev. Lett. **94**, 157205 (2005).
[25] J. Sugiyama (unpublished).
[26] K. Nishiyama, S. Ohira, W. K. Dawson, and W. Higemoto, Hyperfine Interact. **104**, 349 (1997).
[27] A. C. Masset, C. Michel, A. Maignan, M. Hervieu, O. Toulemonde, F. Studer, B. Raveau, and J. Hejtmanek, Phys. Rev. B **62**, 166 (2000).
[28] Y. J. Uemura, W. J. Kossler, X. H. Yu, J. R. Kempton, H. E. Schone, D. Opie, C. E. Stronach, D. C. Johnston, M. S. Alvarez, and D. P. Goshorn, Phys. Rev. Lett. **59**, 1045 (1987).
[29] L. P. Le *et al.*, Phys. Rev. B **53**, R510 (1996).
[30] G. M. Kalvius, D. R. Noakes, and O. Hartmann, *Handbook on the Physics and Chemistry of Rare Earths* (North-Holland, Amster-

dam, 2001), Vol. 32.
[31] A. T. Savici *et al.*, Phys. Rev. B **66**, 014524 (2002).
[32] Y. J. Uemura, *Muon Science* (Institute of Physics, Bristol, 1999).
[33] T. Fukai, Y. Furukawa, S. Wada, and K. Miyatani, J. Phys. Soc. Jpn. **63**, 4067 (1996).
[34] V. A. M. Brabers and A. D. D. Broemme, J. Magn. Magn. Mater. **104-107**, 405 (1992).
[35] N. Tristan, J. Hemberger, A. Krimmel, J.-A. Krug von Nidda, V. Tsurkan, and A. Loidl, Phys. Rev. B **72**, 174404 (2005).
[36] K. M. Kojima *et al.*, Phys. Rev. Lett. **79**, 503 (1997).
[37] J. Sugiyama, Y. Ikedo, K. Mukai, J. H. Brewer, E. J. Ansaldo, G. D. Morris, K. H. Chow, H. Yoshida, and Z. Hiroi, Phys. Rev. B **73**, 224437 (2006).
[38] D. A. Andreica, Ph.D. thesis, ETH-Zurich, 2001.
[39] W. L. Roth, J. Phys. (Paris) **25**, 507 (1964).
[40] G. Blasse, Phys. Lett. **19**, 110 (1965).
[41] A. Krimmel, M. Mücksch, V. Tsurkan, M. M. Koza, H. Mutka, C. Ritter, D. V. Sheptyakov, S. Horn, and A. Loidl, Phys. Rev. B **73**, 014413 (2006).
[42] J. Sugiyama, C. Xia, and T. Tani, Phys. Rev. B **67**, 104410 (2003).
[43] Y. Miyazaki, M. Onoda, T. Oku, M. Kikuchi, Y. Ishii, Y. Ono, Y. Morii, and T. Kajitani, J. Phys. Soc. Jpn. **71**, 491 (2002).
[44] Y. Miyazaki (private communication).